COBEM 2023 27TH INTERNATIONAL CONGRESS OF MECHANICAL ENGENEERING

ABCM Brazilian Society of Mechanical Sciences and Engineering
27th ABCM International Congress of Mechanical Engineering
December 04-08, 2023, Florianópolis-SC, Brazil

COB-2023-1878
CHARACTERIZATION OF THE AA6082 MATRIX COMPOSITE WITH NbC OBTAINED THROUGH FRICTION STIR PROCESSING

Denner Traiano
Federal University of Technology – Paraná (UTFPR), R. Doutor Washington Subtil Chueire, 330 - Jardim Carvalho, Ponta Grossa - PR, 84017-220
denner_traiano9@outlook.com

Bruno Edu Arendarchuck
Federal University of Technology – Paraná (UTFPR), R. Doutor Washington Subtil Chueire, 330 - Jardim Carvalho, Ponta Grossa - PR, 84017-220
edu9831@hotmail.com

Simone do Rocio Ferraz Sabino
Federal University of Technology – Paraná (UTFPR), R. Doutor Washington Subtil Chueire, 330 - Jardim Carvalho, Ponta Grossa - PR, 84017-220
mone.sb@hotmail.com

Luciano Augusto Lourençato
Federal University of Technology – Paraná (UTFPR), R. Doutor Washington Subtil Chueire, 330 - Jardim Carvalho, Ponta Grossa - PR, 84017-220
lalouren@utfpr.edu.br

Hipolito Domingo Carvajal Fals
Federal University of Technology – Paraná (UTFPR), R. Doutor Washington Subtil Chueire, 330 - Jardim Carvalho, Ponta Grossa - PR, 84017-220
hipolitofals@utfpr.edu.br

Abstract. *Towards the growing need to improve the wear performance and properties of aluminum alloys used in the automotive and industrial sectors, aluminum matrix surface composites (AMCs) have gained attention. Among the chief techniques, Friction stir processing (FSP) has emerged as a promising technology due to its energy efficiency and metallurgical advantages. So, in this work, an aluminum matrix alloy AA6082-T4 surface composite reinforced with niobium carbide (NbC) was obtained by FSP. A 200 µm thick layer of carbides was applied using thermal spraying for further processing. FSP was conducted with a threaded cylindrical pin tool, rotating at 1200 rpm and a feed rate of 40 mm/min. The FSP process involved different quantities of passes and a tilt angle of 2.5° in the feed direction. The samples were characterized using optical microscopy, scanning electron microscopy (SEM), x-ray spectroscopy (EDS), and Vickers microhardness tests. Scratching tests were performed to determine the coefficient of friction (CoF). The AMCs obtained on the base material's surfaces exhibited a reduced Coefficient of Friction (CoF) and improved microstructure with finer grain formation in the modified regions. Overall, it demonstrates the feasibility of using FSP to obtain surface composites and enhance the wear resistance of the AA6082-T4 alloy against friction.*

Keywords: *friction stir processing, aluminum matrix surface composite, niobium carbide, wear, microstructure.*

1. INTRODUCTION

The Friction Stir Processing (FSP) technique has been used as a surface treatment, aiming to improve the surface properties of materials (Zykova et al., 2020; Escobar et al., 2021). Surface modification using FSP promotes large plastic deformation, mechanical mixing, and localized heat. The process occurs through a high-hardness tool, accompanied by high rotation speeds and controlled feed (Fernández et al., 2018; Escobar et al., 2021).

This process focuses on improving the material's surface, considerably reducing grain size and eliminating defects in the treated area. The process occurs with a low influence of heat and high plastic deformation along the surface (Zhang et al., 2012; Sunil, 2019).

In this context, the FSP process offers a notable advantage by eliminating metallurgical issues associated with the liquid phase in fusion welding when working with solid-state materials. Conversely, aluminum alloys, with extensive

applications in sectors like automotive and aerospace, suffer from wear-related challenges, curtailing their utility (Chaudhary et al., 2018). Within this context, the industrial-grade AA6082-T4 aluminum alloy stands out as a significant member of the alloy series.

Numerous investigations were developed to evaluate the effect of applying the FSP process on the microhardness of aluminum alloys AA6082 (Scialpi et al., 2007), AA 6061 (Rodrigues et al., 2009) and AA 6063 (Sato et al., 1999) . In general, the formation of a W-shaped microhardness profile was observed in the cross-section. Hardness values are attributed to grain refinement and dissolution of second-phase precipitates (Mg2Si). An increase in microhardness is observed towards the tool feed side; a certain softening is also observed in the nugget zone (NZ) and minimum microhardness values in the thermomechanically affected zone (TMAZ) on the tool feed side. All these microhardness profile variations are attributed to microstructure variations due to different material flow patterns within the agitation zone.

El-Rayes and El-Danaf (2012) studied the influence of rotation and feed rate and even the number of passes of the FSP process on the surface modification of an AA6082 alloy. It was found that when the number of passes increased, it led to an increase in the grain size in the ZN, plus dissolution and re-precipitation with intense fragmentation of the second-phase particles. On the other hand, increasing the feed rate also reduces the size of the second phase particle and increases the mean of the ultimate tensile strength (UTS) and hardness of nugget zone (NZ). The increase in the tool rotation speed did not influence the NZ's hardness but caused the grains' coarsening.

In order to enhance their mechanical properties, the FSP technique has been employed to produce Aluminum Matrix Composites (AMMC). Recently Sunil (2019) proved that FSP is effective for producing composites. The process allows the distribution of the reinforcements in the matrix. The reinforcement particles can be pre-allocated on the surface through grooves, small holes, the sandwich method, or thermal spraying without altering the material bulk. In the zone modified by plastic deformation, the distribution of reinforcing particles occurs, mainly increasing hardness and wear resistance.

Guo et al. (2016) used the FSP technique with several passes to produce composites of AA6061 with Al_2O_3. A microstructural analysis showed that incorporating reinforcement influenced the grain size decrease. The microhardness and tensile properties of the composites obtained with 4 passes were significantly higher than the base metal, and this improvement was attributed to grain refinement and the inclusion of reinforcements.

Choi et al. (2012), developed a composite material manufactured with SiC particles in AA6061-T4 by FSP. They observed a recrystallized fine-grain structure in the NZ, with the SiC particles homogeneously distributed in the Al matrix. The hardness of the treated zone was improved by reducing grain size and dispersed SiC particles.

Kurtyka et al. (2015) elucidated the impact of plastic deformation induced by FSP on the concentration and distribution of SiC reinforcement particles in the A339/SiC/p cast composite. The authors verified the bands' formation in the SiC reinforcement distribution in the modified zone, obtaining an anisotropic behavior. In this sense, depending on the area examined, compared to the raw material, they obtained an increase of about 40% for compressive strength and 30% for hardness.

In previous studies aimed at enhancing the Friction Stir Processing (FSP) technique, various reinforcement materials such as SiC, Al_2O_3, graphene, graphite, CNT, WS_2, B_4C, graphite, WC, among others were used (Mabuwa et al., 2022). However, the use of NbC is very scarce in the composites' production (Arendarchuck et al., 2022). Only a few investigations have explored the incorporation of NbC in the FSP process. Kumar et al. (2019) utilized small NbC particles (10-20 μm) in an A7075 alloy, albeit with grooves created in the aluminum alloy to accommodate the NbC. Their findings demonstrated an improvement in hardness and UTS.

In this sense, the FSP technique is employed to obtain a surface composite in the A6082-T4 alloy with niobium carbide (NbC) reinforcement, which is applied through thermal spraying. The objective is to evaluate the macrostructural characteristics and distribution of NbC particles and assess the resulting composite's hardness and wear resistance.

2. MATERIALS AND METHODS

Aluminum sheets of AA6082-T4 alloy with dimensions of 150 x 100 x 5 mm were utilized as a raw material for the thermal spraying process. The sheets of AA6082-T4 present a hardness of 85 HV, UTS 205 Mpa, and Yield Tensile Strength of 110 Mpa. Moreover, its chemical composition can be visualized in Table 1.

Table 1. Chemical composition of AA6082 alloy (wt.%)

Al	Cu	Mg	Si	Fe	Mn	Cr	Zn	Ti
95.2-98.3	≤ 0.10	0.60-1.2	0.70-1.3	≤ 0.5	0.4-1.0	≤ 0.25	≤ 0.20	≤ 0.10

Niobium carbide powder (LC-550), provided by the Brazilian Mining and Metallurgy Company (CBMM), was used in this study. The powder had an average grain size of 150 ± 27 μm. A thermal spray process was employed to apply a coating of 200 μm average thickness, analyzed by SEM images, on the surface of AA6082-T4 sheets. Forming the NbC coating, Ni-Al bond coating was applied with a 50 μm average thickness. The application of the NbC coatings was carried

out by OPT Brazil using the Flame Spray process with the TeroDyn System 2000 equipment. The specific parameters of the thermal spray process can be found in Table 2.

Table 2. Thermal spray coating process parameters

Powder flux (g/min)	Stand-off distance (SOD) (mm)	Aspersion angle (°)	Oxygen pressure (psi)	Acetylene pressure (psi)	Air pressure (psi)	Aspersion speed (mm/s)
25	80	90	38	60	60	140

The surface modification of AA6082-T4 sheets and NbC was achieved using a nitrated H13 steel tool. The tool employed in this study was a threaded cylindrical pin with a diameter of 5 mm, a shoulder measuring 20 mm, and a height of 3 mm. The friction stir processing (FSP) was performed on a computer numerical control (CNC) ROMI D machine, with a rotational speed of 1200 rpm and a feed rate of 40 mm/min. The tool tilt angle of 2.5º in the feed direction was maintained constant throughout the process. The experimental conditions included four different scenarios: a single pass, two passes, three passes, and a combination of 1 pass on the clockwise and another on the counterclockwise. A schematic diagram of the process can be visualized in Figure 1.

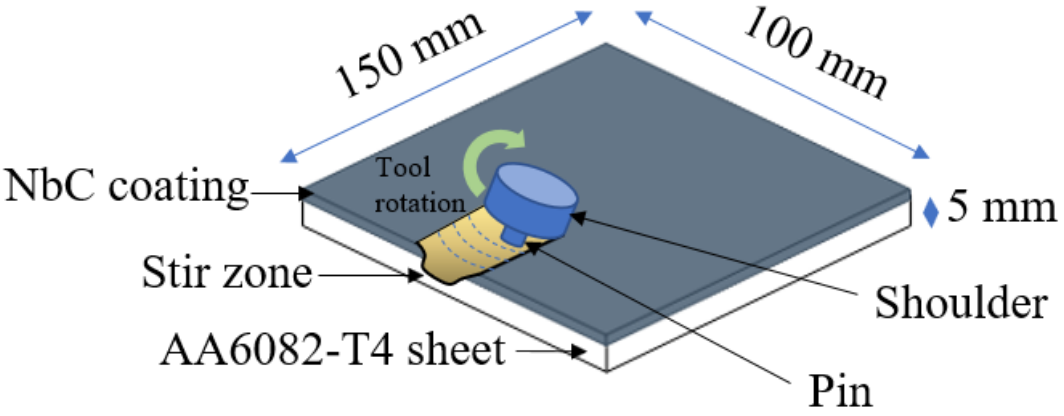

Figure 1. Schematic diagram of the friction stir process of AA6082-T4 matrix with NbC reinforcements

The cross-section of the samples was prepared using a standard metallographic process for micro and macro characterization. Scanning electron microscopy (SEM) were performed using a Tescan Vega 3 along with Energy dispersive X-ray spectroscopy (EDS) analysis of the samples equipment, and Optical microscopy (OM) from Zeiss. The influence of FSP process and the number of the passes on the size of reinforcement particles was analyzed using ImageJ® software and presented in form of histograms.

The samples were subjected to etching with Keller's reagent to assess the grain size structure using polarized images. The etching process involved the use of a 6% fluoboric acid (HBF4) solution in aqueous medium, with a voltage of 25 V and a current of 1.9 A, for a duration of 150s.

Tribometer brand TTP was employed for conducting Coefficient of Friction (CoF) tests. The scratch test method was employed, applying a normal force of 10 N for a duration of 300 seconds, at a frequency of 5 Hz, using AISI 52100 chrome steel spheres. Scratch tests were performed on the base and modified materials after the FSP process.

Hardness was assessed using a Shimadzu Vickers/Knopp microhardness tester under a 300g load. The measurements were taken on the cross-section of the tool's feed and retreat regions in the substrate, as well as in the TMAZ, heat-affected zone (HAZ), and nugget of the modified samples.

3. RESULTS AND DISCUSSION

Figure 2 shows a micrograph of the cross-section of the AA6082-T4 substrate and the coating of the NbC and Ni-Al. It is clear to see the presence of Ni-Al bond coating; this material's choice is due to the promotion an adequate adhesion and uniformity of the NbC. The main objective of the NbC coating is to propitiate the formation of the composite by FSP, and in general, it was observed that the obtained coatings have an average thickness of 150 ± 50 µm, exhibiting a heterogeneous lamellar structure with the presence of interlamellar pores, typical of a thermal spray coating by flame

spray. The defects, such as voids or oxides, present in the coatings do not affect the formation of surface AMCs through friction stir processing

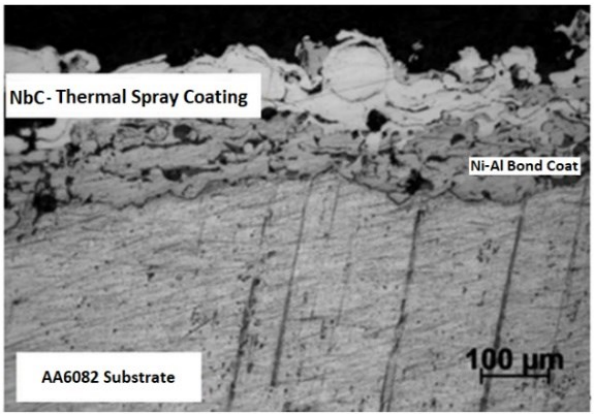

Figure 2. Micrograph of the thermal spray coating of NbC and Ni-Al

Figure 3 (A), provides a detailed view of the cross-section of the sample with 1 pass, highlighting the distinct regions formed during the FSP process, including the heat-affected Zone (HAZ), thermomechanically affected zone (TMAZ), and nugget zone (NZ). The dispersion of NbC particles throughout the material, predominantly in the TMAZ of the retreating zone, is evident.

Examining the impact of the number of passes and particle dispersion, tests were conducted at a feed rate of 40 mm/min and a rotational speed of 1200 rpm. Figure 3 (B) illustrates the surface characteristics of samples subjected to different pass configurations, demonstrating that the resulting AMC zones exhibited uniformity and a defect-free surface. However, burrs were observed at the edges due to plastic deformation caused by the friction of the tool shoulder.

Furthermore, Figure 3 (C) presents cross-sections of various cases, revealing consistent absence of defects such as pores and unfilled regions across different pass configurations. This indicates the robustness of the modified regions regardless of the number of passes.

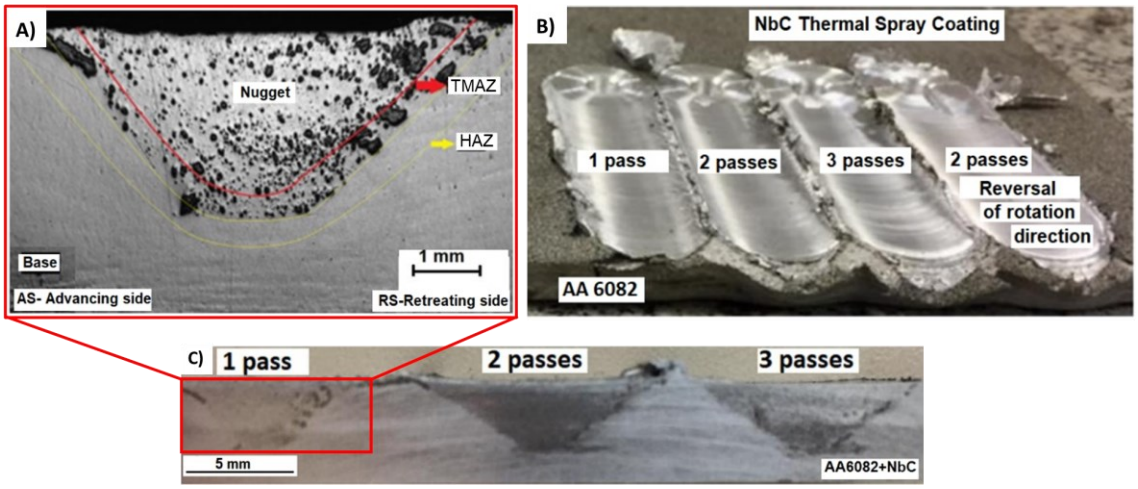

Figure 3. (A) Cross-section of composite with 1 pass with marked zones, (B) photo of the sheet after the FSP process, (C) cross-section of the FSP process passes

To confirm the presence of NbC, EDS analyses were carried out, the elements maps are show in Figure 4. Additionally, a schematic of SEM images was utilized to show the localization of NbC particles, it is observed that the reinforcement particles have various sizes, resulting from the tool effect during the FSP processing of the previously deposited reinforcement layer as a coating. The set of images also highlights a cluster of approximately 150 µm, accurately identified through EDS analysis, where small NbC carbides are observed in the Fe matrix, as indicated by the manufacturer of this material. The images also reveal an adequate metallurgical bonding with the AA6082-T4 alloy matrix and the possible presence of β-Mg2Si second-phase precipitates, which occur in this aluminum alloy.

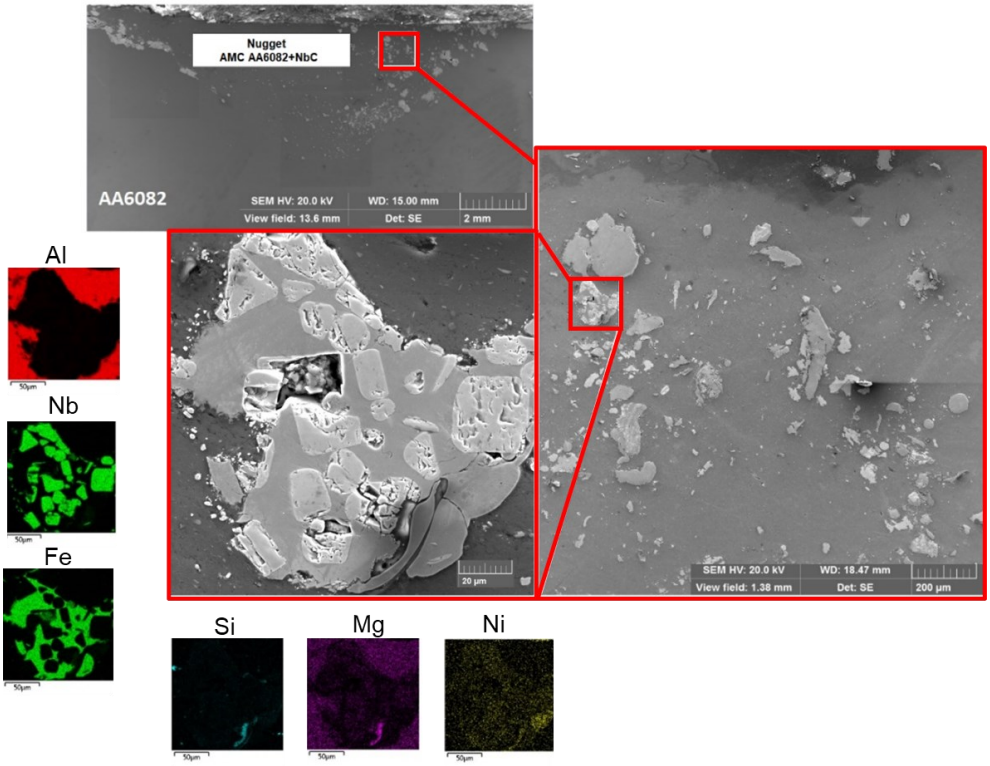

Figure 4. Micrographs of SEM images highlighting the NbC particles in the composites, with EDS elements maps

Figure 5 cross-sectional polarized optical micrographs,shows the modified region of the AA6082-T4+NbC composite obtained by FSP with 1 pass . The image provides a detailed visualization of the microstructure in both the feed and retreating sides of the HAZ and TMAZ.

In qualitative visualizations, there is an expressive grain size reduction in the TMAZ and NZ areas compared to the AA6082-T4 substrate. The grains tend to become equiaxial in this region due to the thermomechanical regime imposed during the FSP process inducing grain recrystallization. The formation of deformation bands, commonly called "onion rings" in the literature, is also observed. These regions exhibit significant differences in crystal orientation between the feed and retreating zones of the TMAZ, resulting from the type and state of deformation occurring in the material flow induced by the tool geometry.

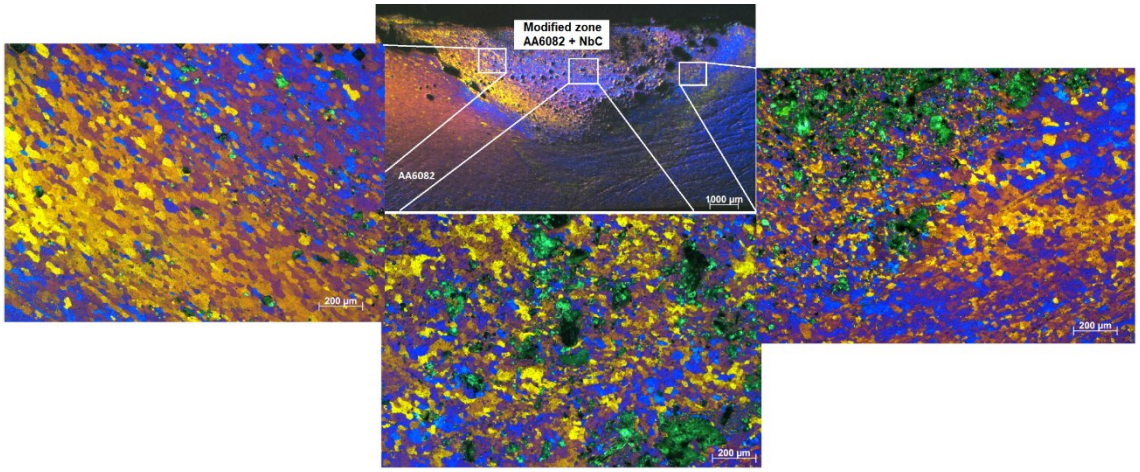

Figure 5. Optical micrographs of NZ cross-section of the AA6082-T4+NbC with 1 pass

A visual reduction in grain size was noticed by increasing the number of passes. Comparing Figure 6, which shows the composite with 3 passes, with Figure 5 this reduction can be verified. Similar results were found by Bikkina et al.

(2020), where a grain size reduction was observed with pass number increase. They attribute the grain size reduction to recrystallization and inhibited grain growth due to NbC particles, acting as effective sites for grain nucleation.

Generally, FSP tends to change to grains almost equixially, and the thermomechanical forces tend to promote a grain size reduction, which probably supports the subsequent results.

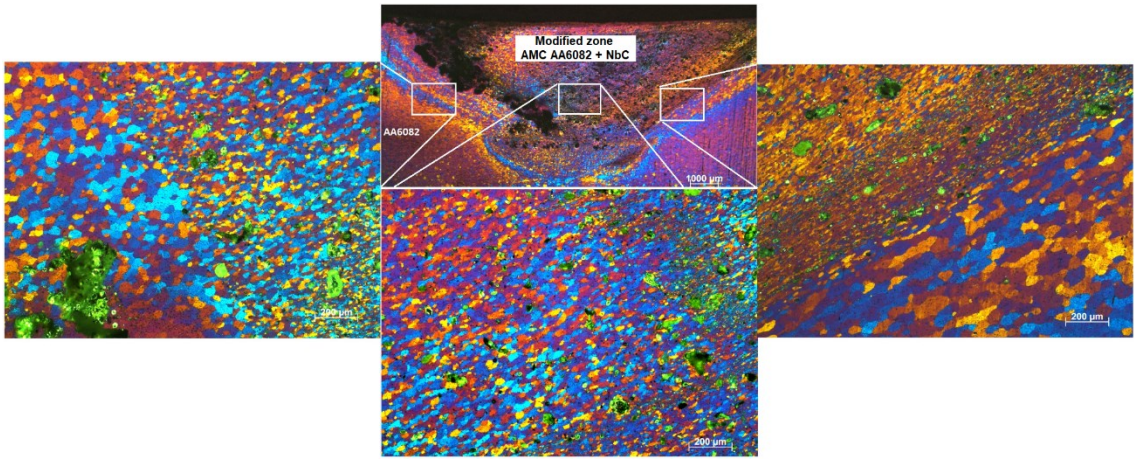

Figure 6. Optical micrographs of NZ cross-section of the AA6082-T4+NbC with 3 passes

3.1 Analysis of reinforcements' size and distribution

In Figure 7, the utilized scheme for determining the average area of NbC particles is presented. Optical images reveal the presence of clusters in the TMAZ zone under all conditions, primarily on the retreating side with 2 passes and on the feeding side with 3 passes. The histogram analysis indicates a significant variation in particle area for the FSP with one pass. Conversely, the condition with 2 passes exhibits a reduction in area accompanied by an increased number of particles, as observed in the image analysis. The sample with 3 passes demonstrates greater uniformity in particle area, possibly due to cluster fragmentation resulting from the additional pass.

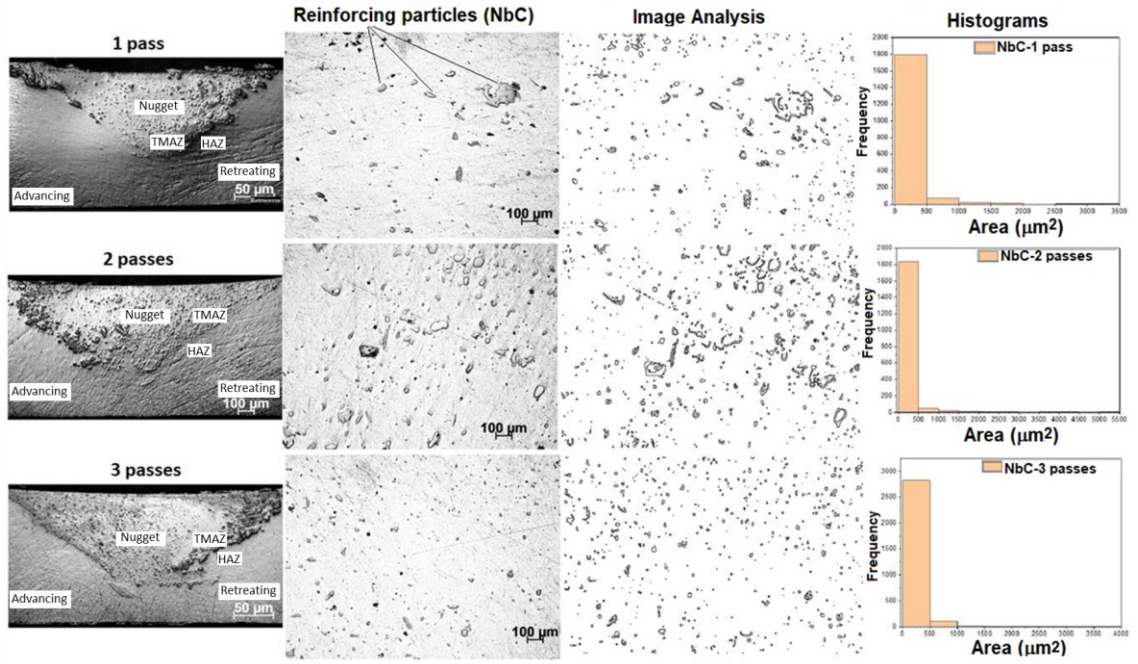

Figure 7. Representative scheme of the process utilized to determine the average area of the NbC particles

Figure 8 provides a close-up of the condition involving one clockwise pass and one subsequent counterclockwise pass. This setup significantly reduces the particle area, resulting in smaller particles than other setups. However, it also leads to the formation of clusters, mainly on the feed side. However, it also leads to the formation of clusters, mainly on the feed side. Furthermore, the image shows a central defect that triggers the collapse of the nugget.

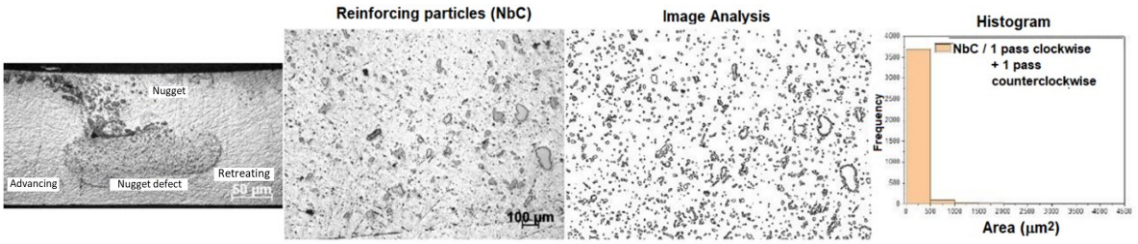

Figure 8. Scheme demonstration the decreased average area of NbC particles in a test with one clockwise pass, followed by an additional counterclockwise pass.

The modified zone undergoes significant microstructural changes through the FSP process, which are affected by chemical composition, process parameters, and substrate condition. FSP also directly impacts on mechanical properties such as hardness, which is linked to factors like part geometry, quantity of reinforcement particles, and dispersion. Thus, the following section will discuss the analysis of hardness results.

3.2 Hardness measurements

Vickers microhardness were performed in the HAZ, TMAZ and nugget zone, The results are presented in Figure 9, showing a gradual increase in hardness in both the HAZ and TMAZ with an increasing number of passes. However, in the nugget zone, a reduction in hardness was observed when analyzing the test with 3 passes. This can be attributed to the elevated temperature during this pass, which causes the thickening of precipitates and directly impacts the hardness results.

The sample subjected to an additional counterclockwise pass exhibited higher hardness, measuring 137 HV_{300}. This could be attributed to improved NbC dispersion and the possible influence of a nugget defect, leading to microstructural alterations that contributed to the increased hardness.

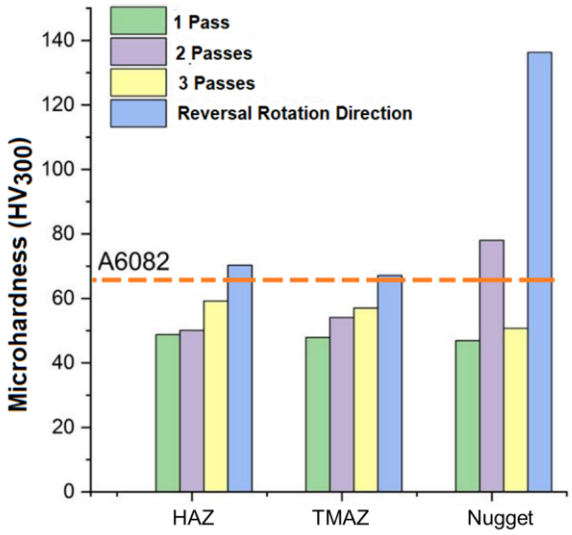

Figure 9. Microhardness results of the HAZ, TMAZ and nugget zone of FSP samples with varying numbers of passes

The reference hardness value of the AA6082-T4substrate is represented by the horizontal line in the graph. The majority of HAZ and TMAZ values are below this threshold. However, samples with extra reversal rotation direction exhibit slightly higher values in the HAZ and TMAZ, with a significant increase in the NZ. Moreover, the condition involving 2 passes shows hardness levels above the substrate in the nugget region.

The FSP process induces severe plastic deformation and generates heat through friction, leading to the formation of equiaxed microstructures with smaller grains due to recrystallization. In this scenario, the reduction in hardness may be attributed to solubilization and coarsening of precipitates, which are associated with secondary hardening of the alloy, as

well as the limited influence of NbC particles in cases where cluster formations occur. This scenario is more evident in the TMAZ zone due to the concentration of the cluster in this area.

3.3 Coefficiente of friction analysis

Application of FSP process leads to microstructural changes that influence the wear properties. The CoF of the samples were analyzed and results were plotted in a graph in Figure 10, showing CoF for AA6082-T4 substrate and (B) for composite with 3 passes.

In the case of the substrate (the initial CoF value was higher and gradually decreased, stabilizing after 100s, with an average value of 0.62 ± 0.08. Conversely, in (B) a significant reduction in CoF values is evident, reaching an average value of 0.47 ± 0.09, a reduction of 24.2 %.

In the substrate case (Figure 10 (A)), the initial CoF value started high and gradually decreased, stabilizing around 0.62 ± 0.08 after 100 seconds. In contrast, Figure 10 (B) shows a noticeable decrease in CoF values, averaging at 0.47 ± 0.09, marking a 24.2% reduction. Several factors contribute to this reduction.

The FSP process induces grain refinement, enhancing hardness and lowering CoF. NbC particles also raise hardness by acting as barriers against dislocations, fostering smaller grains during recrystallization. These particles serve as load-bearing barriers, lessening direct abrasive-substrate contact and wear. Moreover, as explained by Sharma et al. (2020) the presence of reinforcements may curtail groove formation along wear paths, minimizing material loss and wear mechanisms like abrasion and adhesion, ultimately reducing CoF.

Chaudhary et al. (2018), in their review on composites produced by solid-state techniques, similarly emphasized that reinforcement addition and increasing FSP process passes correlate with CoF reduction through these mechanisms.

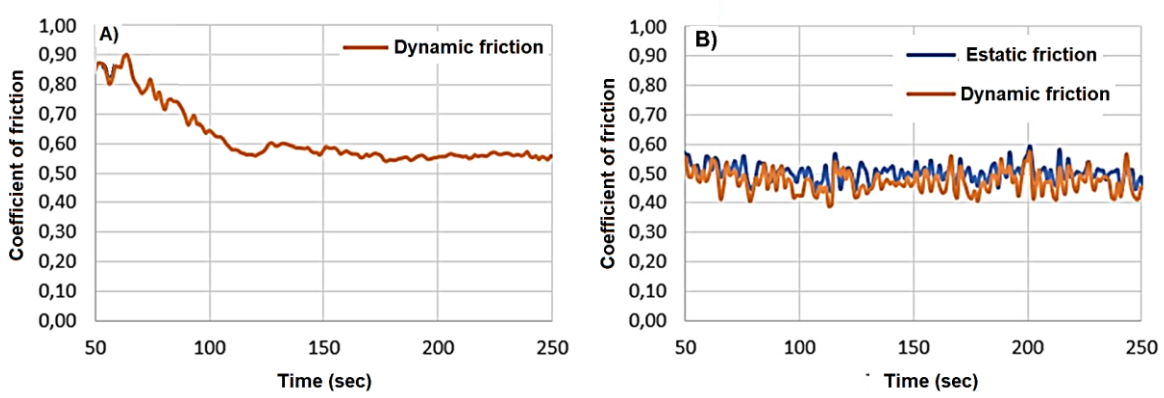

Figure 10. (A) AA6082-T4 coefficient of friction (CoF), (B) CoF of the composite with 3 passes

4. CONCLUSIONS

The successful application of the FSP process on NbC-coated AA6082-T4 has demonstrated the impact of different numbers of passes on the microstructure, hardness, and wear characteristics of the composite. In summary, the following conclusions can be drawn:

- The utilization of the thermal spray coating proved effective and viable in introducing reinforcement for subsequent FSP processing.
- Application of FSP process induced microstructural changes in the AA6082-T4 substrate, resulting in recrystallized equiaxed grains. The distribution of NbC particles was facilitated by FSP, with cluster formations primarily observed in the retreating zone of TMAZ.
- The main parameter analyzed in this work, the number of the passes emerged as a crucial parameter, impacting particle dispersion and size. The increased number of passes improved NbC distribution, generally resulting in smaller grain sizes. Although in the condition with 1 pass for each rotational direction, there was a collapse defect in the NZ.
- In the HAZ and TMAZ, the modified zone with 1, 2, or 3 passes exhibited a reduction in hardness compared to the AA6082-T4 substrate, likely attributed to solubilization, coarsening of precipitates, and limited influence of NbC particles in the presence of cluster formations. Nonetheless, the scenario involving one clockwise pass followed by an additional counterclockwise pass exhibited higher average values compared to the substrate.
- A reduction of 24.2% in CoF was obtained by adding NbC in the AA6082-T4 substrate by FSP process (with 3 passes). Which is very important to increase product life when exposed to wear mechanisms.

5. ACKNOWLEDGEMENTS

The authors would like to thank Technological Federal University of Paraná (UTFPR). The National Council for Scientific and Technological Development (CNPq)/Araucaria Foundation for aid in promotion and (C2MMa) Lab for the analyses conducted. Special thanks are also extended to CBMM for supplying the NbC powder. Additionally, the Coordination for the Improvement of Higher Education Personnel (CAPES) in Brazil is acknowledged for providing financial support for this study (Financing Code 001).

6. REFERENCES

Arendarchuck, B. E.; Fals, H. D. C.; Lourençato, L. A., 2022, Effect of Thixoforming Process and Microstructural Changes in the A380 Matrix Composite Reinforced with NbC by the Stir Casting Method,JOM, Vol.75, pp.184–194.
Bikkina, V.; Talasila, S. R.; Adepu, K., 2020, Characterization of aluminum based functionally graded composites developed via friction stir processing,Transactions of Nonferrous Metals Society of China, Vol.30, pp.1743–1755.
Chaudhary, R.; Joshi, S.; Singh, R. C., 2018, Mechanical and wear performance of surface composite fabricated by solid-state Technique-A review,Materials Today: Proceedings, Vol.5, pp.28033–28042.
Choi, D. H.; Kim, Y. I.; Kim, D. U.; Jung, S. B., 2012, Effect of SiC particles on microstructure and mechanical property of friction stir processed AA6061-T4,Transactions of Nonferrous Metals Society of China, Vol.22, pp.s614–s618.
El-Rayes, M. M.; El-Danaf, E. A., 2012, The influence of multi-pass friction stir processing on the microstructural and mechanical properties of Aluminum Alloy 6082,Journal of Materials Processing Technology, Vol.212, pp.1157–1168.
Escobar, J.; Gwalani, B.; Olszta, M.; Silverstein, J.; Overman, N.; Bergmann, L.; dos Santos, J. F.; Staron, P.; Maawad, E.; Klusemann, B.; Mathaudhu, S.; Devaraj, A., 2021, Multimodal analysis of spatially heterogeneous microstructural refinement and softening mechanisms in three-pass friction stir processed Al-4Si alloy,Journal of Alloys and Compounds, Vol.887, pp.161351.
Fernández, C. M. A.; Rey, R. A.; l Ortega, M. J. C.; Verdera, D.; Vidal, C. L., 2018, Friction stir processing strategies to develop a surface composite layer on AA6061-T6,Materials and Manufacturing Processes, Vol.33, pp.1133–1140.
Guo, J.; Lee, B. Y.; Du, Z.; Bi, G.; Tan, M. J.; Wei, J., 2016, Effect of Nano-Particle Addition on Grain Structure Evolution of Friction Stir-Processed Al 6061 During Postweld Annealing,JOM, Vol.68, pp.2268–2273.
Kumar, T. S.; Suganya Priyadharshini, G.; Shalini, S.; Krishna Kumar, K.; Subramanian, R., 2019, Characterization of NbC-reinforced AA7075 alloy composites produced using friction stir processing,Transactions of the Indian Institute of Metals, Vol.72, pp.1593–1596.
Kurtyka, P.; Rylko, N.; Tokarski, T.; Wójcicka, A.; Pietras, A., 2015, Cast aluminium matrix composites modified with using FSP process – Changing of the structure and mechanical properties,Composite Structures, Vol.133, pp.959–967.
Mabuwa, S.; Msomi, V.; Ndube-Tsolekile, N.; Zungu, V. M., 2022, Status and progress on fabricating automotive-based aluminium metal matrix composites using FSP technique,Materials Today: Proceedings, Vol.56, pp.1648–1652.
Rodrigues, D. M.; Loureiro, A.; Leitao, C.; Leal, R. M.; Chaparro, B. M.; Vilaça, P., 2009, Influence of friction stir welding parameters on the microstructural and mechanical properties of AA 6016-T4 thin welds,Materials & Design, Vol.30, pp.1913–1921.
Sato, Y. S.; Kokawa, H.; Enomoto, M.; Jogan, S., 1999, Microstructural evolution of 6063 aluminum during friction-stir welding,Metallurgical and Materials Transactions A: Physical Metallurgy and Materials Science, Vol.30, pp.2429–2437.
Scialpi, A.; De Filippis, L. A. C.; Cavaliere, P., 2007, Influence of shoulder geometry on microstructure and mechanical properties of friction stir welded 6082 aluminium alloy,Materials & Design, Vol.28, pp.1124–1129.
Sharma, A.; Fujii, H.; Paul, J., 2020, Influence of reinforcement incorporation approach on mechanical and tribological properties of AA6061- CNT nanocomposite fabricated via FSP,Journal of Manufacturing Processes, Vol.59, pp.604–620.
Sunil, B. R., 2019, *Surface Engineering by Friction-Assisted Processes* 1st edn. Apple Academic Press, Boca Raton, Florida.
Zhang, Y. N.; Cao, X.; Larose, S.; Wanjara, P., 2012, Review of tools for friction stir welding and processing,Canadian Metallurgical Quarterly, Vol.51, pp.250–261.
Zykova, A.; Chumaevskii, A.; Gusarova, A.; Kalashnikova, T.; Fortuna, S.; Savchenko, N.; Kolubaev, E.; Tarasov, S., 2020, Microstructure of In-Situ Friction Stir Processed Al-Cu Transition Zone,Metals, Vol.10.

7. RESPONSIBILITY NOTICE

The authors are the only responsible for the printed material included in this paper.